Fizika Nizkikh Temperatur, 2001, v. 27, No. 4, p. 385–391

Effect of oxygen content on magnetization and magnetoresistance properties of CMR manganites

S. V. Trukhanov, I. O. Troyanchuk, and F. P. Korshunov

Institute of Solid State and Semiconductor Physics of National Academy of Sciences of Belarus, 17 P. Brovki Str., Minsk 220072, Belarus
E-mail: troyan@ifttp.bas-net.by

V. A. Sirenko

B. Verkin Institute for Low Temperature Physics and Engineering of the National Academy of Science of Ukraine 47 Lenin Ave., Kharkov 61164, Ukraine

H. Szymczak

Institute of Physics of Polish Academy of Sciences, 32/46 Al. Lotnikow Str., 02-668 Warsaw, Poland

K. Baerner

Physikalisches Institut der Universitat Goettingen, 11-15 Bunsenstr., 37073 Goettingen, Germany

Received 26 October, 2000

The influence of oxygen content on the magnetization and electrical resistivity of $Ln_{0.5}A_{0.5}MnO_3$ (Ln = La, Pr, Nd; A = Ca, Ba) manganites with the perovskite structure is investigated. It is shown that the $La_{0.5}Ca_{0.5}MnO_{3-\gamma}$ compound undergoes a sequence of transitions from an antiferromagnetic ($\gamma = 0$) to a spin-glass ($\gamma = 0.17$) state and then to an inhomogeneous ferromagnetic ($\gamma = 0.3$) state. A transition from an antiferromagnetic charge-ordered state to a ferromagnetic charge-disordered state in $Nd_{0.5}Ca_{0.5}MnO_{3-\gamma}$ is observed as the oxygen content is reduced to where $\gamma = 0.07$. The $Nd_{0.5}Ba_{0.5}MnO_{3-\gamma}$ compound shows an increase of the Curie point from 110 K ($\gamma = 0$) up to 310 K ($\gamma = 0.3$). In addition, a large magnetoresistance is revealed which develops below their Curie temperature despite the absence of Mn^{3+}–Mn^{4+} pairs. A Zener double-exchange interaction is usually used in literature to explain the magnetic and electrical properties of hole-doped perovskite manganites. The data obtained support the mechanism of superexchange interactions between magnetic moments of the manganese ions via oxygen.

PACS: 75.30.Vn, 75.30.Cr

1. Introduction

The manganites $Ln_{1-x}A_xMnO_3$ (Ln = La, Nd, Pr etc., A = Ca, Sr, Ba etc.) with the perovskite structure are representative of the material class known to show an interesting interplay between magnetic, orbital, and charge ordering as well as electrical transport [1–3]. These compounds were already known at the very early stage of the experimental [4] and theoretical [5] study on transition metal oxides. However, their «renaissance» has been sparked by the discovery of the magnetic-field-induced insulator–metal [6,7] and charge order–disorder [8] transitions.

The issue of charge ordering in perovskite manganites has attracted a considerable attention during the last few years after discovery of the so-called «colossal» magnetoresistance (CMR) effect [8]. There are different CMR effects in manganites. One of them arises near T_C in ferromagnetic samples and is associated with an insulator-metal transition, another is due to a «melting» of the charge-ordered state in an external magnetic field and is associated with a charge order–disorder transition [9,10]. The charge ordering phenomenon was studied for the first time in $La_{0.5}Ca_{0.5}MnO_3$ by Wollan and Koehler [11] and Goodenough [12].

$La_{0.5}Ca_{0.5}MnO_3$ is a paramagnetic semiconductor above $T_C \approx 225$ K and transforms to a charge-

ordered antiferromagnetic semiconductor ($T_N \approx 180$ K) phase (CE type) through an incommensurate ferromagnetic semiconductor phase. It is notable that this compound has antiferromagnet–ferromagnet and charge order–disorder transitions at the same temperature ($T_N = T_{co}$). $Nd_{0.5}Ca_{0.5}MnO_3$ is paramagnetic semiconductor above the corresponding Néel temperature ($T_N \approx 180$ K) and transforms directly to the charge-ordered antiferromagnetic semiconductor phase (CE type) through a charge-ordered paramagnetic semiconductor phase ($T_{co} \approx \approx 260$ K). The critical temperature T_{co} of the charge ordering is well above the magnetic ordering temperature T_N , and the two transitions are clearly decoupled [13]. Neither of the above-mentioned compositions displays an insulator–metal transition. They are semiconductors in the whole temperature range.

The $Ln_{0.5}Ba_{0.5}MnO_3$ perovskites are much less studied. However, it is well known that they do not exhibit antiferromagnet–ferromagnet and charge order–disorder transitions. It was found that $La_{0.5}Ba_{0.5}MnO_3$ is a ferromagnet with $T_C \approx 340$ K [14]. The $Pr_{0.5}Ba_{0.5}MnO_3$ and $Nd_{0.5}Ba_{0.5}MnO_3$ have Curie points of 125 K [15] and 120 K [16], respectively. These compositions have an insulator–metal transition near T_C and a magnetoresistance peak slightly below T_C .

In order to explain the appearance of the ferromagnetism in hole-doped perovskites and connection between the antiferromagnet–ferromagnet and insulator–metal transitions, Zener has introduced a special form of the exchange interactions via carriers — double exchange (DE) [17]. De Gennes developed this theory and predicted that a noncolinear magnetic structure forms at intermediate concentrations between the antiferromagnetic and ferromagnetic states [18].

It has been established that the magnetic and electrical transport properties of the manganites depend markedly on oxygen content. Both the Curie point and magnetization decrease, whereas the resistivity increases with increasing oxygen deficit [19]. Nevertheless, the influence of oxygen content on the insulator–metal and charge order–disorder transitions is not well studied to date.

In view of what we have said, in this paper we report the results of an investigation of the effect of oxygen content on the magnetization and magnetoresistance properties of $Ln_{0.5}A_{0.5}MnO_{3-\gamma}$ (Ln = = La, Nd, Pr; A = Ca, Ba). The measurements reveal many interesting features. As we will see, the data obtained could be used to support the superexchange interaction scenario of ferromagnetic ordering in manganites, in contrast to DE theory.

2. Experiment

The $Ln_{0.5}A_{0.5}MnO_3$ (Ln = La, Nd, Pr; A = Ca, Ba) compounds were prepared by standard solid-state reaction from powders of Ln_2O_3 , ACO_3 , and Mn_2O_3 taken in designed ratios. After prefiring at 727 °C the mixtures were pressed in the form of discs and sintered at T = 1550 °C for 2 h in air. After synthesis the samples were annealed at 900 °C for 100 h in air and slowly cooled at a rate of 100 °C·h^{-1} to room temperature in order to obtain the oxygen stoichiometric compounds. The synthesized samples were checked for phase purity and lattice parameters by powder x-ray diffraction (XRD) with a DRON-3 diffractometer in CoK_α radiation. The XRD patterns were collected in the angle range of $20° \le 2\theta \le 80°$. The oxygen content of sintered samples was determined by a thermogravimetric analysis. These investigations showed that the oxygen content is stoichiometric. The as-prepared samples were reduced using different methods. The Ca series of samples were treated in evacuated silica tubes at T = 850°C for during 2 h using metallic tantalum as a getter. The reduction for the Ba series was made in flowing argon under a carbon crucible at 880°C for 30 h. These reduction reactions can be described by the relation

$$Ln_{1-x}Ca_xMnO_3 + (2\gamma/5)\ Ta \rightarrow$$

$$\rightarrow Ln_{1-x}Ca_xMnO_{3-\gamma} + (\gamma/5)\ Ta_2O_5\ . \qquad (1)$$

The following values of oxygen deficit were obtained: $0 \le \gamma \le 0.5$ for the $La_{0.5}Ca_{0.5}MnO_{3-\gamma}$, and $0 \le \gamma \le 0.2$ for $Nd_{0.5}Ca_{0.5}MnO_{3-\gamma}$ samples. The oxygen deficit of the reduced samples was calculated from the change of weight of the samples during reduction. We did not observe any appreciable changes in the weight of $Pr_{0.5}Ba_{0.5}MnO_3$ and $Nb_{0.5}Ba_{0.5}MnO_3$ samples during reduction. The relative error of the oxygen content measurements does not exceed 1%. Therefore, the chemical formula of the reduced samples may be written as a $Ln_{1-x}A_xMnO_{3-\gamma\pm0.02}$.

The magnetization measurements were made using an OI-3001 vibrating-sample magnetometer in the temperature range 4–350 K. The electrical resistivity measurements were performed by a standard four-probe method using ultrasonically deposited indium contacts. The magnetoresistance was calculated according to the relation

$$MR = \left\{ \frac{\rho(H) - \rho(H = 0)}{\rho(H = 0)} \right\} \cdot 100\ \%\ , \qquad (2)$$

where MR is the magnetoresistance, $\rho(H)$ is the resistivity in a magnetic field of 9 kOe, and $\rho(H = 0)$ is the resistivity in the absence of magnetic field.

3. Results and discussion

The XRD patterns of the samples show them to be nominally single-phase with the perovskite structure. The unit cell parameters are listed in the Table. The symmetry of the unit cell for the $Ln_{1-x}Ba_xMnO_{3-\gamma}$ samples is cubic. The $Ln_{1-x}Ca_xMnO_{3-\gamma}$ samples exhibit the small so-called O-orthorombic distortions ($a < c\sqrt{2} < b$) [20] which are due to the mismatch between the ionic sizes of different ions. Generally speaking, the majority of the hole-doped perovskite manganites show lattice distortions as modifications from the cubic structure. One of the distortions is the deformation of the MnO_6 octahedron arising from the Jahn–Teller effect, which is peculiar to the high-spin ($S = 2$) Mn^{3+} ions. Another comes from the size effect because of the mismatch between the sizes of ions and the interstices occupied by them in the perovskite lattice. In this case the MnO_6 octahedron is rotated around the cubic axes, lowering the lattice symmetry from the cubic. The rotation around the [100] axis corresponds to tetragonal distortions, around [110] — to orthorhombic and [111] — to rhombohedral ones. In the samples with doping ion content above $x \geq 0.1$ the static Jahn–Teller distortions are eliminated and the crystal structure distortions are determined by the size effect, which is observed in our case. The magnitude of these distortions increases with increasing deviation from oxygen stoichiometry. The volume of the unit cell for reduced samples is greater than that for oxidized ones. The volume change arises from the removal of the oxygen ions and the conversion Mn^{4+} to Mn^{3+}. It seems reasonable to propose that the increase of the volume is due to the conversion of the small Mn^{4+} ions to the relatively large Mn^{3+} ones. The effective ionic radii of Mn^{3+} and Mn^{4+} in octahedral oxygen coordination are 0.390 E and 0.830 E, respectively [21].

Table

Symmetry (O — O-orthorombic, C — cubic), the unit cell parameters a, b, c and the volume V of the $Ln_{0.5}A_{0.5}MnO_{3-\gamma}$ (Ln = La, Pr, Nd; A = Ca, Ba) manganites with different oxygen content

Composition	Symmetry	a, Å	b, Å	c, Å	V, Å^3
$La_{0.5}Ca_{0.5}MnO_3$	O	5.397	5.442	7.659	224.95
$La_{0.5}Ca_{0.5}MnO_{2.83}$	O	5.412	5.467	7.675	227.08
$La_{0.5}Ca_{0.5}MnO_{2.7}$	O	5.425	5.484	7.688	228.72
$Nd_{0.5}Ca_{0.5}MnO_3$	O	5.375	5.421	7.635	222.47
$Nd_{0.5}Ca_{0.5}MnO_{2.93}$	O	5.382	5.433	7.641	223.43
$Pr_{0.5}Ba_{0.5}MnO_3$	C	3.900			59.30
$Pr_{0.5}Ba_{0.5}MnO_{3-\gamma}$	C	3.889			58.80
$Nd_{0.5}Ba_{0.5}MnO_3$	C	3.891			58.92
$Nd_{0.5}Ba_{0.5}MnO_{3-\gamma}$	C	3.892			58.97

The $M(T)$ curves for the $La_{0.5}Ca_{0.5}MnO_{3-\gamma}$ samples in a magnetic field of 11 kOe are displayed in Fig. 1. On warming the stoichiometric compound exhibits an enhancement and a drop of the magnetization at 160 and 260 K, respectively. In agreement with published data, the anomalous behavior around 160 K is associated with an antiferromagnet–ferromagnet transition, whereas at 260 K there is the Curie point. The magnetic behavior of the phase with $\gamma = 0.17$ is incompatible with ferromagnetic behavior because its magnetic moment ($\mu \approx 0.33$ μ_B/f.u. at 6 K) is much less than that expected for ferromagnetic ordering of all the Mn-ion magnetic moments. The value of the magnetic moment per ($Mn^{3+}_{0.84}Mn^{4+}_{0.16}$) unit calculated from a pure ionic model is 3.8 μ_B/f.u. ($\mu(Mn^{3+}) \approx 4\ \mu_B$ and $\mu(Mn^{4+}) \approx 3\ \mu_B$). Both a small magnetic moment and broad transition to the magnetically disordered state are consistent with an inhomogeneous magnetic state.

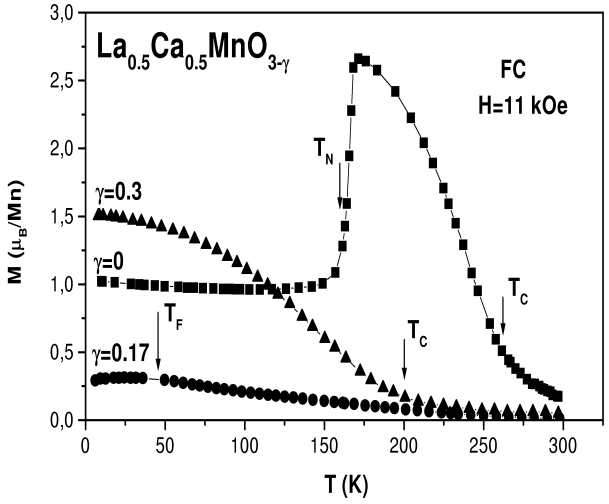

Fig. 1. Magnetization of the $La_{0.5}Ca_{0.5}MnO_{3-\gamma}$ ($\gamma = 0$, 0.17, 0.3) samples in a magnetic field of 11 kOe as a function of temperature.

Such behavior of magnetization is typical for the spin glasses, where magnetic clusters of magnetic moments are gradually blocked with decreasing temperature. The surprise is that the magnetization increases strongly when the content of oxygen vacancies becomes equal 0.3, i.e., almost all the manganese ions adopt the tri-valent state. However, the magnetic moment at 6 K is only 1.5 μ_B per manganese ion, whereas for the ferromagnetically ordered phase the expected value is 4.1 μ_B/f.u.

The ferromagnetism in the manganites is usually explained in terms of the DE interaction with the transfer of an electron from the Mn^{3+} to the Mn^{4+} ions [17]. However, in the framework of this model it is impossible to understand the ferromagnetic properties of the manganites not containing Mn^{4+} ions [20,22–23]. Goodenough [20] has adduced arguments for the ferromagnetism in the manganites to be due not only to double exchange but also to the specific character of the exchange interactions in the Jahn–Teller Mn^{3+} ion system. He has proposed that the orbital configuration of the 3*d* electrons while removing the static Jahn–Teller distortions is determined by the position of the ions' nuclei. In this case the dynamic enhancement of the ferromagnetic part of exchange interactions at the expense of correlation in the orbital orientation of neighboring ions must occur (Goodenough's quasistatic hypothesis). According to the superexchange mechanism an exchange between Mn^{3+} and Mn^{4+} depends on a number of factors: Mn–O bond distance, Mn–O–Mn bond angle [23], Mn^{3+}–Mn^{4+} ratio (the nearer it is to 1, the more intensive the exchange), etc. It is known that Mn^{4+}–O–Mn^{4+} interactions are always antiferromagnetic while Mn^{3+}–O–Mn^{3+} interactions in octahedral coordination are magnetically anisotropic in the orbital ordered phase (ferromagnetic in one direction and antiferromagnetic in others) and isotropic in the orbital disordered phase (ferromagnetic) [20]. It is also known that sign of superexchange interactions Mn^{3+}–O–Mn^{3+} depends on the anion environment. In the case of fivefold coordination these interactions became antiferromagnetic [24]. Taking all this into account led us to be guided by the superexchange interaction mechanism for as complete as possible a description of the magnetization and resistivity properties of the perovskite manganites.

At the oxygen vacancy concentration $\gamma = 0.17$ in the $La_{0.5}Ca_{0.5}MnO_{3-\gamma}$ samples the antiferromagnetic exchange interactions dominate due to the strong negative Mn^{3+} (6-fold coordination) –O–Mn^{3+} (5-fold coordination) superexchange interaction. The magnetization data for the strongly reduced sample ($\gamma = 0.3$) led us to propose that the oxygen vacancies are distributed nonrandomly over the crystal lattice, making up an oxygen-vacancy superstructure. This is very likely because it is established from the selected area electron diffraction measurements [25] that the difference between $La_{0.5}Ca_{0.5}MnO_3$ and $La_{0.5}Ca_{0.5}MnO_{2.75}$ structures is that the size of the microdomains is much smaller in the latter compound. It is therefore proposed that the anion defects in the $La_{0.5}Ca_{0.5}MnO_{2.75}$ structure seem to be accommodated in the form of clusters in the domain walls. This is reasonable because with the domain size decreasing as the concentration of the oxygen vacancies increases, the domain surface diminishes more slowly than the domain volume. In the oxygen-vacancy superstructure case the positive superexchange interactions Mn^{3+} (6-fold coordination) –O–Mn^{3+} (6-fold coordination) in the $La_{0.5}Ca_{0.5}MnO_{2.7}$ may be dominant, thus leading to ferromagnetic properties.

In Fig. 2 the data from the magnetization measurements are shown versus temperature in a magnetic field of 14.8 kOe for $Nd_{0.5}Ca_{0.5}MnO_{3-\gamma}$ with $\gamma = 0$ and 0.07. The stoichiometric sample exhibits a magnetization peak at T = 260 K. From published data it is known this peak is due to charge ordering. This sample does not go to a ferromagnetic state on cooling. It becomes a charge-ordered antiferromagnet directly, even though the 1:1 ratio of Mn^{3+}/Mn^{4+} ions is one of the favorable conditions for DE interactions. The sample with $\gamma = 0.07$ exhibits a sharp enhancement of the magnetization at 105 K. The magnetic moment $\mu \approx 2.1$ μ_B/f.u. at 10 K is less than expected value 3.2 μ_B/f.u. This magnetic anomaly can be understood from the discussion below. The appearance of the Mn^{3+} excess leads to

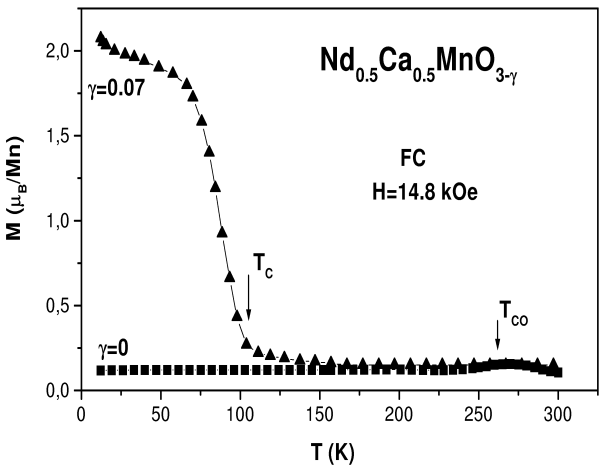

Fig. 2. Magnetization curves versus temperature for the $Nd_{0.5}Ca_{0.5}MnO_{3-\gamma}$ samples with $\gamma = 0$ and 0.07 in a magnetic field of 14.8 kOe.

reinforcement of the ferromagnetic superexchange interactions because of the breaking of the Mn^{3+}/Mn^{4+} location symmetry and consequently of the charge ordering. However, the homogeneous ferromagnetic state is not realized, because of the strong negative Mn^{3+} (6-fold coordination) $-O-Mn^{3+}$ (5-fold coordination) superexchange interactions present. This sample consists of a ferromagnetic medium and antiferromagnetic clusters with short-range order of the magnetic moments. It is appropriate to recall that the substitution of Fe, Ti, Al, Co and Ni for a fraction of the Mn ions also leads to the destruction of the charge ordering; nevertheless, the ferromagnetic state is not realized without an external magnetic field [26].

The stoichiometric $Pr_{0.5}Ba_{0.5}MnO_3$ and $Nd_{0.5}Ba_{0.5}MnO_3$ samples are characterized by T_C = = 160 K, $\mu \approx 2.6\ \mu_B/Mn$ at 5 K and T_C = 110 K, $\mu \approx 2.2\ \mu_B/Mn$ at 5 K, respectively (Fig. 3). Surprisingly, the Curie points are much lower than that of $La_{0.5}Ba_{0.5}MnO_3$ (T_C = 340 K) [14]. The relatively low magnetic moment may be attributed to a canted magnetic state or to a mixture of two magnetic phases. In the last case some part of the sample would be ferromagnetic whereas another would be antiferromagnetic. It is impossible to distinguish these situations on the basis of the magnetization data only. However, neutron magnetic resonance experiments for hole-doped manganites with low dopant level have been interpreted in terms of a mixed magnetic state [27]. Neutron diffraction [11] and high-resolution electron microscopy [28] results also support this point of view. We can therefore assume that the stoichiometric samples are magnetically inhomogeneous and contain some antiferromagnetic domains. In addition, the boundary of the concentration ferromagnet–antiferromagnet transition in $Ln_{1-x}Ba_xMnO_3$ is very close to $x = 0.5$ [16].

Curiously enough, the reduced $Pr_{0.5}Ba_{0.5}MnO_{3-\gamma}$ and $Nd_{0.5}Ba_{0.5}MnO_{3-\gamma}$ samples are magnetically ordered up to 310 K (Fig. 4). Thus the Curie point for these compounds has increased by about three times after reduction. These data are very interesting because reduced perovskite manganites have never displayed an increase of the magnetic ordering temperature to date. These reduced samples are also inhomogeneous, since they have $\mu \approx$ 40.4 emu/g at 5 K and $\mu \approx$ 48.6 emu/g at 27 K for $Pr_{0.5}Ba_{0.5}MnO_{3-\gamma}$ and $Nd_{0.5}Ba_{0.5}MnO_{3-\gamma}$, respectively, which are smaller than for the parallel orientation of the magnetic moments ($\mu \approx 4\ \mu_B/Mn$ and $\mu \approx 4.1\ \mu_B/Mn$). The data obtained lead us to propose that either the oxygen coordination of the manganese ion majority is close to six in the reduced samples or the exchange between Mn^{3+} (6-fold coordination) and Mn^{3+} (5-fold coordination) may be positive. It is very likely the first possibility is realized as a result of the oxygen vacancies ordering. In support of this we can recall the new ordered oxygen-deficient perovskite $LaBaMn_2O_{5.5}$, which has been synthesized using the topotactic deoxygenation of the ordered $LaBaMn_2O_6$ perovskite [29]. However, we have not any direct demonstration of the fact of oxygen ordering in our compound. It is necessary to undertake a structural study to verify the eventual crystal structure peculiarities of these reduced samples.

$Pr_{0.5}Ba_{0.5}MnO_{3-\gamma}$ shows a high resistivity ρ in comparison with the oxidized sample (Fig. 5,*a*). It

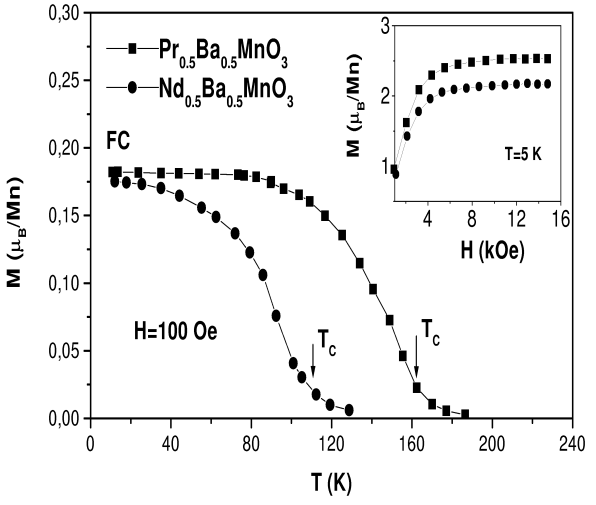

Fig. 3. Field-cooling magnetization versus temperature in a magnetic field of 100 Oe for the stoichiometric $Pr_{0.5}Ba_{0.5}MnO_3$ and $Nd_{0.5}Ba_{0.5}MnO_3$ samples. The inset shows the field dependences of the same compounds at 5 K.

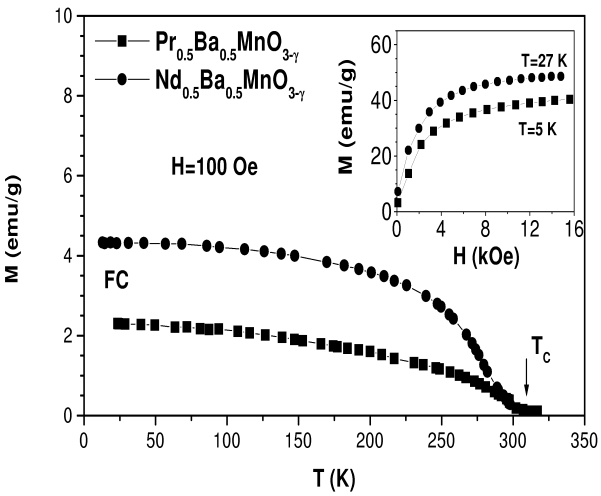

Fig. 4. Field-cooling magnetization versus temperature in magnetic field of 100 Oe for the reduced $Pr_{0.5}Ba_{0.5}MnO_{3-\gamma}$ and $Nd_{0.5}Ba_{0.5}MnO_{3-\gamma}$ samples. The inset shows the field dependences of the same compounds at 5 and 27 K, respectively.

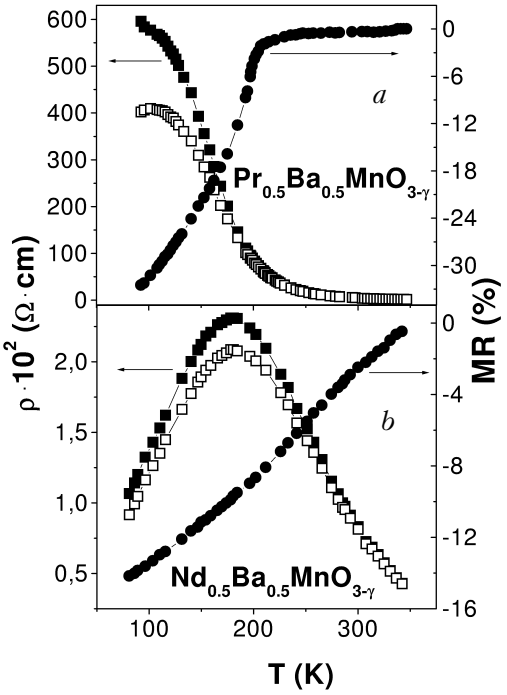

Fig. 5. Electrical resistivity (❐ — $H = 9$ kOe, ■ — $H = 0$) and magnetoresistance (●) for the $Pr_{0.5}Ba_{0.5}MnO_{3-\gamma}$ (*a*) and $Nd_{0.5}Ba_{0.5}MnO_{3-\gamma}$ (*b*) samples versus temperature.

is known $Pr_{0.5}Ba_{0.5}MnO_3$ has a resistivity of about 10 Ω·cm, a metal–insulator transition at 125 K, and a peak of magnetoresistance reaching 47% at 120 K [15]. The value of resistivity in the so-called metallic state (at low temperature) is considerably higher than Mott's value of the maximal metallic resistivity. The peak of the magnetoresistivity being slightly below their Curie temperature is very typical for the hole-doped manganites. The resisitivity of the reduced $Pr_{0.5}Ba_{0.5}MnO_{3-\gamma}$ is about 10^5 Ω·cm, without any transitions down to liquid nitrogen temperatures. The reduced sample remains an insulator in the whole region 77–350 K. Its magnetoresistance hasn't any peak and starts to develop at 200 K. There is no appreciable magnetoresistance effect for the high-temperature ferromagnetic phase. Around liquid nitrogen temperature the magnetoresistance reaches 33% in a field of 9 kOe. In Fig. 5,*b* the resistivity and magnetoresistance are shown for $Nd_{0.5}Ba_{0.5}MnO_{3-\gamma}$ compound. The resistivity is about 100 Ω·cm. The metal–insulator transition temperature is 180 K. The magnetoresistance of this sample has no peak and reaches 14% at 80 K. The magnetoresistance values of the reduced samples are comparable with those for the best samples of the $Sr_2(FeMo)O_6$ system [30]. The resistivity of these reduced samples can be understood assuming that it is determined by the ratio Mn^{3+}/Mn^{4+} and that oxygen bridges are present through which the electron hopping is realized. Hence decreasing this ratio and the oxygen content leads to an increase of the resistivity. The resistivity of the stoichiometric $Nd_{0.5}Ba_{0.5}MnO_3$ is larger than for $Pr_{0.5}Ba_{0.5}MnO_3$ [16]. In the case of the presence of Mn^{2+} the number of oxygen vacancies is too large, but we suppose that the low resistivity of the reduced $Nd_{0.5}Ba_{0.5}MnO_{3-\gamma}$ with respect to $Pr_{0.5}Ba_{0.5}MnO_{3-\gamma}$ can result from the more inhomogeneous distribution of the oxygen vacancies over the sample volume. This possibility is also confirmed by the lower magnetic moment value for $Pr_{0.5}Ba_{0.5}MnO_{3-\gamma}$ than for $Nd_{0.5}Ba_{0.5}MnO_{3-\gamma}$, although before the reduction it was otherwise (Figs. 3 and 4).

The above-described measurements have brought out many interesting features which cannot be explained by DE theory. The data obtained could be used to support the superexchange interaction mechanism of manganese magnetic moments in manganites, in contrast to DE theory. In order to understand the magnetization and electrical resistivity properties of the reduced samples we have assumed a nonrandom distribution of the oxygen vacancies in the crystal lattice. Certainly, further crystal and magnetic structure refinements are needed, including by the powder neutron diffraction and high, resolution electronic microscopy methods, for a better-understanding of the properties of the reduced perovskite manganites.

Acknowledgments

This work was supported in part by the Belarus Fund of Fundamental Research (F98-056).

1. H. W. Hwang, S.-W. Cheong, P. G. Radaelli, M. Marezio, B. Batlogg, *Phys. Rev. Lett.* **75**, 914 (1995).
2. A. P. Ramirez, P. Schiffer, S.-W. Cheong, C. H. Chen, W. Bao, T. T. M. Plastra, P. L. Gammel, D. J. Bishop, and B. Zegarski, *Phys. Rev. Lett.* **76**, 3188 (1996).
3. W. Bao, J. D. Axe, C. H. Chen, and S.-W. Cheong, *Phys. Rev. Lett.* **78**, 543 (1997).
4. C. W. Searle and S. T. Wang, *Can. J. Phys.* **47**, 2023 (1969).
5. K. Kubo and N. Ohata, *J. Phys. Soc. Jpn.* **33**, 21 (1972).
6. K. Chabara, T. Ohno, M. Kasai, and Y. Kozono, *Appl. Phys. Lett.* **63**, 1990 (1993).
7. R. von Helmolt, J. Wocker, B. Holzapfel, M. Schultz, and K. Samwer, *Phys. Rev. Lett.* **71**, 2331 (1993).
8. Y. Tomioka, A. Asamitsu, Y. Moritomo et al., *Phys. Rev. Lett.* **74**, 5108 (1995).
9. P. G. Radaelli, D. E. Cox, M. Marezio, and S.-W. Cheong, *Phys. Rev.* **B55**, 3015 (1997).
10. Y. Tomioka, A. Asamitsu, H. Kuwahara, Y. Moritomo, and Y. Tokura, *Phys. Rev.* **B53**, 1689 (1996).
11. E. O. Wollan and W. C. Koehler, *Phys. Rev.* **100**, 545 (1955).
12. J. B. Goodenough, *Phys. Rev.* **100**, 564 (1995).

13. S. Krupicka, M. Marysko, Z. Jirak, and J. Hejtmanek, *JMMM* **206**, 45 (1999).
14. F. Millange, V. Caignaert, B. Domenges, B. Raveau, and E. Suard, *Chem. Mater.* **10**, 1974 (1998).
15. I. O. Troyanchuk, S. V. Trukhanov, H. Szymczak, and K. Baerner, *J. Phys.: Condens. Matter* **12**, L155 (2000).
16. I. O. Troyanchuk, D. D. Khalyavin, S. V. Trukhanov, and H. Szymczak, *J. Phys.: Condens. Matter* **11**, 8707 (1999).
17. C. Zener, *Phys. Rev.* **82**, 403 (1951).
18. P.-G. De Gennes, *Phys. Rev.* **118**, 141 (1960).
19. H. L. Ju, J. Gopalakrishnan, J. L. Peng, Qi Li, G. C. Xiong, T. Venkatesan, and R. L. Greene, *Phys. Rev.* **B51**, 6143 (1995).
20. J. B. Goodenough, A. Wold, R. J. Arnot, and N. Menyuk, *Phys. Rev.* **124**, 373 (1961).
21. R. D. Shanon, *Acta Crystallogr.* **A32**, 751 (1976).
22. I. O. Troyanchuk, D. D. Khalyavin, E. F. Shapovalova et al., *Phys. Rev.* **B58**, 2422 (1998).
23. E. E. Havinga, *Philips Res. Rep.* **21**, 432 (1966).
24. K. R. Poeppelmeier, M. E. Leonowicz, and J. M. Longo, *J. Solid State Chem.* **44**, 89 (1982).
25. J. M. Gonzalez-Calbet, E. Herrero, N. Rangavittal, J. M. Alonso, J. L. Martinez, and M. Vallet-Regi, *J. Solid State Chem.* **148**, 158 (1999).
26. B. Raveau, A. Maignan, and C. Martin, *J. Solid State Chem.* **130**, 162 (1997).
27. G. Allodi, R. De Renzi, G. Guidi, F. Licci, and M. W. Pieper, *Phys. Rev.* **B56**, 6036 (1997).
28. A. Moreo, S. Yunoki, and E. Dagotto, *Science* **283**, 2034 (1999).
29. V. Caignaert, F. Millange, B. Domenges, and B. Raveau, *Chem. Mater.* **11**, 930 (1999).
30. T. H. Kim, M. Uehara, and S.-W. Cheong, *Appl. Phys. Lett.* **74**, 1737 (1999).